

Nanoscale observation of room-temperature ferromagnetism on ultrathin (La,Ba)MnO₃ films

Teruo Kanki, Run-Wei Li, and Yasuhisa Naitoh

Institute of Scientific and Industrial Research, Osaka University, 8-1 Mihogaoka, Ibaraki, Osaka, 567-00476 Japan

Hidekazu Tanaka

Institute of Scientific and Industrial Research, Osaka University, 8-1 Mihogaoka, Ibaraki, Osaka, 567-00476 Japan and PRESTO, Japan Science and Technology Corporation, Japan

Takuya Matsumoto and Tomoji Kawai^{a)}

Institute of Scientific and Industrial Research, Osaka University, 8-1 Mihogaoka, Ibaraki, Osaka, 567-00476 Japan

(Received 30 April 2003; accepted 9 June 2003)

We have fabricated La_{0.8}Ba_{0.2}MnO₃ ultrathin films with an atomically flat surface and have systematically investigated the magnetism for film thickness dependence. The 20-nm-thick film showed a maximum peak of T_C (310 K). It was found that even the 5-nm-thick film showed a T_C of 290 K near room temperature, which opens up the possibility of spin devices working at room temperature. Furthermore, we have adopted noncontact magnetic force microscopy to evaluate local magnetization in ultrathin (La,Ba)MnO₃ films, and confirmed that several tens of nanoscale ferromagnetic domains appear at room temperature. © 2003 American Institute of Physics. [DOI: 10.1063/1.1599971]

Perovskite manganese oxide is a well-known carrier-induced ferromagnet that shows ferromagnetism above room temperature,¹ while typical dilute magnetic semiconductors (DMS) (In,Mn)As² and (Ga,Mn)As³ show the Curie temperature (T_C) up to 50 and 110 K, respectively, but not at RT. Recently, some RT ferromagnetic semiconductors, such as Co-doped TiO₂,⁴ Co-doped ZnO,⁵ and Mn- or Cr-doped GaN^{6,7} have been reported, but it remains unclear whether the observed ferromagnetism originated from itinerant carriers or the segregation of nanoclusters of magnetic impurities.^{8,9} Thus, perovskite manganese oxide is one of the best candidates for the realization of RT spin electronic devices. Nevertheless, serious problems remain that prevent these devices from working at RT. The T_C of the well-known (La,Sr)MnO₃ and (La,Ca)MnO₃ are strongly suppressed with decreasing film thickness, due to lattice mismatch^{10,11} and/or the presence of dead layers.^{12,13} Such phenomena are also seen in typical DMS (Ga,Mn)As, whose ferromagnetism disappears below 6.5-nm-thick film.¹⁴ Only in (In,Mn)As did the ferromagnetism survive down to 5 nm thickness.¹⁵ In term of application to devices, for example, in the advanced demonstration using this DMS (In,Mn)As, Ohno's group reported on the electric field control of ferromagnetism in a 5-nm-thick (In,Mn)As thin film field-effect transistor at 22.5 K through carrier modulation.¹⁶ In the practical applications of this technique, RT ferromagnetism is strongly desired, especially in the form of ultrathin films. We have previously reported the enhancement of T_C up to RT in (La,Ba)MnO₃ thin films with 400 to 20 nm thickness, but it was still too thick for device applications. In this letter, we report the magnetic properties of lightly doped (La,Ba)MnO₃ thin films down to 5 nm. Moreover, we characterize nanoscale ferro-

magnetic domain evaluation by using frequency shift mode magnetic force microscopy with high resolution.

The La_{0.8}Ba_{0.2}MnO₃ (LBMO) thin films were deposited on etched perovskite SrTiO₃(001) single-crystal substrates using a pulsed laser deposition (PLD) technique (ArF excimer: $\lambda=193$ nm). SrTiO₃ is the standard substrate used for the deposition of functional perovskite compounds and has the advantages that it is commercially available, has a large dielectric constant,¹⁷ is an *n*-type semiconductor with La or Nb doping,¹⁸ and has epitaxial growth directly on Si.¹⁹ The SrTiO₃ substrates were etched by immersion in a pH-controlled solution of NH₄-HF (pH=5.0), and whose surfaces were then smoothed.^{20,21} The target employed was a sintered LBMO pellet prepared by a conventional solid reaction process. LBMO films were deposited at a substrate temperature of 630 °C in NO₂ at a pressure of 1.0×10^{-4} mbar with the observation of reflection high-energy electron diffraction (RHEED) oscillation. After film formation, the films were annealed at 750 °C for 10 h in an O₂ atmosphere at 1 atm. The film structures were examined by x-ray diffraction and high-resolution transmission electron microscopy (HRTEM, JEOL JEM 3000FIS, operating at 300 kV). The magnetizations of bulk LBMO and the thin films were measured using a superconducting quantum interference device (SQUID) magnetometer. The local magnetizations of LBMO thin films were observed by frequency shift noncontact magnetic force microscopy (NC-MFM, JEOL JSPM-4200) using a ferromagnetic Co-Cr coating cantilever.

Figure 1(a) shows an atomic force microscopic (AFM) image of the LBMO surface (with a film thickness of 12 nm). The width of atomically flat terraces was approximately 150 nm, and the step height was approximately 0.4 nm, corresponding to one unit cell of LBMO. Figure 1(b) shows a typical cross-sectional HRTEM image of a LBMO thin film, demonstrating the sharp film-substrate interface (indicated

^{a)}Author to whom correspondence should be addressed; electronic mail: kawai@sanken.osaka-u.ac.jp

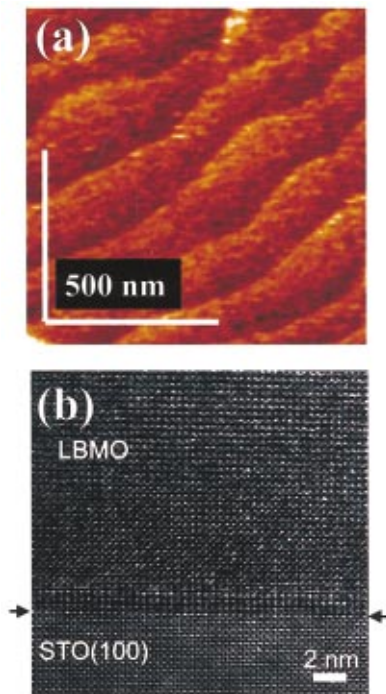


FIG. 1. (Color) (a) AFM image of the epitaxial LBMO thin film on a SrTiO₃(001) substrate. The average height is 0.44 nm, almost corresponding to one LBMO unit cell, and the rms roughness is 0.14 nm. (b) Cross-section TEM image of the film and substrate. The arrow indicates the film-substrate interface.

by the arrow) without any secondary phases. No defects or dislocations of stacking faults were observed. The RHEED images of the thin films showed clear streak patterns, suggesting good crystalline and flat surfaces. These observations confirmed the high crystalline quality and perfect epitaxy of the LBMO thin films.

Figure 2 shows the thickness dependence of T_C of LBMO films expanded to an ultrathin region. The T_C values systematically increased from 270 K (corresponding to the T_C of the bulk sample) to 310 K from 390 to 20 nm with decreasing system thickness. This phenomenon of increased T_C is peculiar to the La_{1-x}Ba_xMnO₃ ($0.05 \leq x \leq 0.2$) system, as reported by our previous papers.^{22,23} On the other hand, in <20-nm-thick films, T_C decreased with decreasing thickness. However, even the 5-nm-thick film still showed a T_C of 290

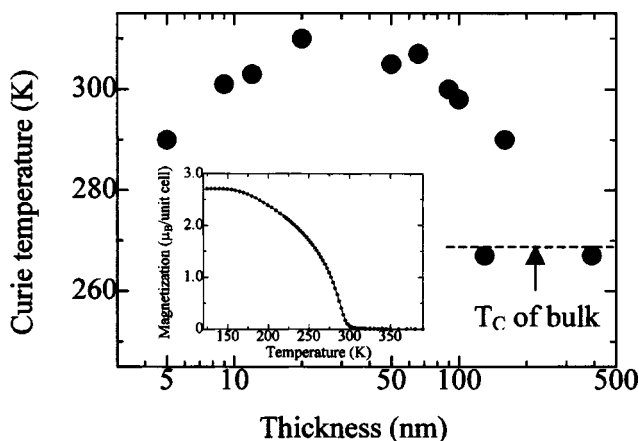


FIG. 2. The thickness dependence of T_C in LBMO films. The inset is the temperature dependence of magnetization of a 5-nm-thick film.

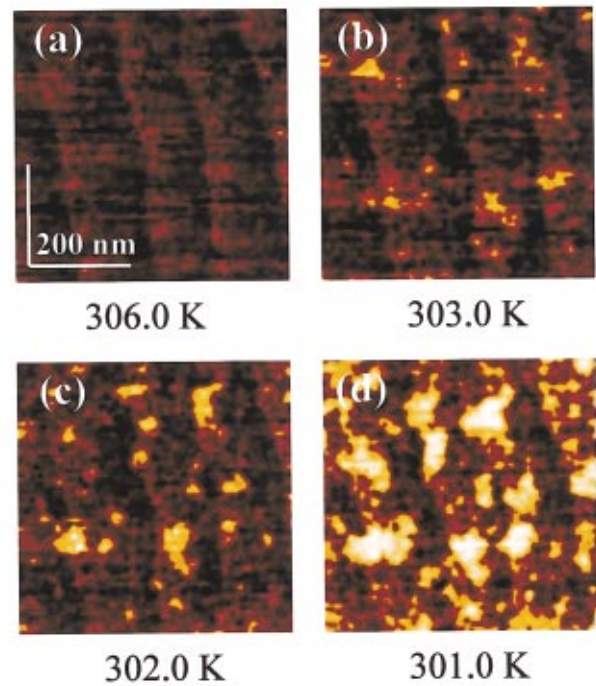


FIG. 3. (Color) The temperature-dependent NC-MFM image sequence for cooling. The rms roughnesses are (a) 0.156 nm at 306 K, (b) 0.191 nm at 303 K, (c) 0.223 nm at 302 K, and (d) 0.267 nm at 301 K, respectively.

K near RT. Showing a higher value than bulk T_C ($=270$ K). It is significant to have achieved RT ferromagnetism in the LBMO films with low doping carriers and less thickness for spintronic applications.

In addition, the evaluation of nanoscale magnetism appearing at the surface or interface is also important for the development of device applications, especially in film with nanometer scale or magnetic nanostructure, in which it is often difficult to decide magnetic state by using a SQUID magnetometer or other devices. In techniques used for the detection of local magnetism, MFM is one of the leading tools. There are many reports in which perovskite manganite thin films²⁴⁻²⁷ have been examined; however, their measurements near T_C were not detailed, which would be important in the case of ferromagnetic switching at RT. And the observed magnetic domains were large, with sizes ranging from several hundred nanometers to micrometers. On the other hand, true atomic-scale resolution was achieved for well-defined clean surfaces by NC-AFM using high-resolution frequency shift spectroscopy,²⁸⁻³⁰ which is able to detect quite weak forces. We have adopted this method of MFM using a ferromagnetic cantilever to the atomically flat LBMO thin film around T_C .

Figure 3 shows the temperature dependence of local magnetic domain behavior around the T_C of the LBMO film with a T_C of 303 K. The height of their MFM images contains both surface morphology (the van der Waals force) and magnetic force. In the case of the temperature dependence, the surface morphology remained unchanged. Only the magnetic force changed, reflecting the magnitude of sample magnetization. No magnetic domains existed above the T_C [Fig. 3(a)]. Only an atomically flat terrace with one-unit-cell steps of the LBMO surface can be confirmed. With decreasing temperature, the magnetic domains with 20 nm width appear at the flat terraces structure at the T_C [Fig. 3(b)]. Further-

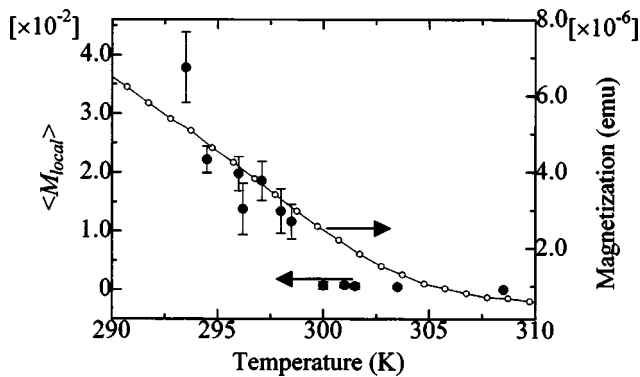


FIG. 4. Temperature dependence of local magnetization led from MFM images and the magnetization measured by SQUID (the solid line). The heights for each temperature were investigated at five different areas, of which dispersions are indicated by error bars.

more, the magnetic domains grow up to 200 nm at 301 K with cooling, as shown in Figs. 3(c) and 3(d). By using the NC-MFM system, the appearance of RT ferromagnetism at the nanoscale level was also confirmed over the entire film surface. Such magnetic domain behavior significantly affects the transport property.^{31–33} In particular, in order to explain the transport property near the metal–insulator transition temperature, a two-phase system formed by the main paramagnetic matrix with insulating conduction and the minor ferromagnetic domains with the metallic one is often invoked, in which the connection of their magnetic domains induces metallic conduction, a so-called percolative conduction that will affect the operation of the devices.

Our attention next turned towards the evaluation of nanoscale magnetisms. In the simplest case, the magnetic force (F_m) is expressed as $F_m \propto M_{tip} M_{sample} / r^2$, where M_{tip} and M_{sample} represent the magnetizations of a tip and LBMO sample, respectively, and r is the distance between the tip and sample surface. Since F_m is fixed by feedback regulation and M_{tip} is a constant parameter, the sample magnetization is proportional to r^{-2} . Therefore, we can estimate local magnetization from the height of their MFM images. Here, the average local magnetization ($\langle M_{local}(T) \rangle$) is given as $\langle M_{local}(T) \rangle \propto [\langle r(T) \rangle - \langle r_{n.m.} \rangle]^2$, where $\langle r(T) \rangle$ is the average height of each MFM image defined as $\langle r \rangle \equiv \sum_i (r_i / s_i) s_i$ represents one pixel of the MFM image and the investigated size corresponds to $\sum_i s_i$, which is 800 nm \times 800 nm at each temperature. $\langle r_{n.m.} \rangle$ is the average height of the paramagnetic image at 308 K, reflecting topographic information. We investigated five different areas. Figure 4 shows the temperature dependence of the local magnetization ($\langle M_{local} \rangle$). The $\langle M_{local} \rangle$ derived from MFM images corresponds to the magnetization curve reflecting the macro scale as measured by SQUID (the solid line). The spread of error bars suggests that the magnetization values differ at each local region. We believe that the observation of nanoscale magnetic domain behavior makes it possible to create workable spintronic devices using a perovskite system, and that NC-MFM techniques will be also applicable to decide the magnetic state of nanostructural devices.

In conclusion, we have created LBMO thin films with atomically flat surfaces that displayed RT ferromagnetism down to 5-nm-thick films on a SrTiO₃(001) substrate according to the PLD technique. In addition, we evaluated the

local surface magnetism in LBMO thin films and succeeded in the detection of small magnetic domain behavior around T_C using NC-MFM. The $\langle M_{local} \rangle$ temperature dependence increased below T_C , which corresponds to the macroscopic magnetization measured by SQUID. This result supports the likelihood of creating RT spintronic devices such as field-effect transistors controlling ferromagnetism by light and electric fields.

- ¹A. Urushibara, Y. Moritomo, T. Arita, A. Asamitsu, G. Kido, and Y. Tokura, Phys. Rev. B **51**, 14103 (1995).
- ²H. Munekata, H. Ohno, S. von Molnar, A. Segmuller, L. L. Chang, and L. Esaki, Phys. Rev. Lett. **63**, 1849 (1989).
- ³H. Ohno, A. Shen, F. Matsukura, A. Oiwa, A. Endo, S. Katsumoto, and Y. Lye, Appl. Phys. Lett. **69**, 363 (1996).
- ⁴Y. Matsumoto, M. Murakami, T. Shono, T. Hasegawa, T. Fukumura, M. Kawasaki, P. Ahmet, T. Chikyow, S. Koshihara, and H. Koinuma, Science **291**, 854 (2001).
- ⁵K. Ueda, H. Tabata, and T. Kawai, Appl. Phys. Lett. **79**, 988 (2001).
- ⁶S. Sonoda, S. Shimizu, T. Sasaki, Y. Yamamoto, and H. Hori, J. Cryst. Growth **237**, 1358 (2002).
- ⁷M. Hashimoto, Y.-K. Zhou, M. Kanamura, and H. Asahi, Solid State Commun. **122**, 37 (2002).
- ⁸D. H. Kim, J. S. Yang, K. W. Lee, S. D. Bu, T. W. Hoh, S.-J. Oh, Y.-W. Kim, J.-S. Chung, H. Tanaka, H. Y. Lee, and T. Kawai, Appl. Phys. Lett. **81**, 2421 (2002).
- ⁹K. Ando, cond-mat/0208010.
- ¹⁰R. A. Rao, D. Lavric, T. K. Nath, C. B. Eom, L. Wu, and F. Tsui, Appl. Phys. Lett. **73**, 3294 (1998).
- ¹¹R. B. Praus, B. Leibold, G. M. Gross, and H.-U. Habermeier, Appl. Surf. Sci. **138–139**, 40 (1999).
- ¹²J. Z. Sun, D. W. Abraham, R. A. Rao, and C. B. Eom, Appl. Phys. Lett. **74**, 3017 (1999).
- ¹³M. Bibes, M.-J. Casanove, Ll. Balcells, S. Valencia, B. Martínez, J.-C. Ousset, and J. Fontcuberta, Appl. Surf. Sci. **188**, 202 (2002).
- ¹⁴T. Hayashi, M. Tanaka, K. Seto, T. Nishinaga, H. Shimada, and K. Ando, J. Appl. Phys. **83**, 6551 (1998).
- ¹⁵H. Munekata, A. Zaslavsky, P. Fumagalli, and R. J. Gambino, Appl. Phys. Lett. **63**, 2929 (1993).
- ¹⁶H. Ohno, D. Chiba, F. Matsukura, T. Omiya, E. Abe, Y. Ohno, and K. Ohtani, Nature (London) **408**, 944 (2000).
- ¹⁷A. Linz, Jr., Phys. Rev. **91**, 753 (1953).
- ¹⁸H. P. R. Frederikse, W. R. Thurber, and W. R. Hosler, Phys. Rev. **134**, A442 (1964); H. Tanaka, J. Zhang, and T. Kawai, Phys. Rev. Lett. **88**, 027204 (2002).
- ¹⁹R. A. McKee, F. J. Walker, and M. F. Chisholm, Phys. Rev. Lett. **81**, 3014 (1998).
- ²⁰M. Kawasaki, K. Takahashi, T. Maeda, R. Tsuchiya, M. Shinohara, O. Ishiyama, T. Yonezawa, M. Yoshimoto, and H. Koinuma, Science **266**, 1540 (1994).
- ²¹G. Koster, G. Rijnders, D. H. A. Blank, and H. Rogalla, Physica C **339**, 215 (2000).
- ²²J. Zhang, H. Tanaka, T. Kanki, J.-H. Choi, and T. Kawai, Phys. Rev. B **64**, 184404 (2001); T. Kanki, H. Tanaka, and T. Kawai, Solid State Commun. **114**, 267 (2000).
- ²³T. Kanki, H. Tanaka, and T. Kawai, Phys. Rev. B **64**, 224418 (2001).
- ²⁴Q. Lu, C.-C. Chen, and A. de Lozanne, Science **276**, 2006 (1997).
- ²⁵Y.-A. Soh, G. Aeppli, N. D. Mathur, and G. Blamire, J. Appl. Phys. **87**, 6743 (2000).
- ²⁶Y.-R. Ma, C.-H. Chueh, W.-L. Kuang, Y. Liou, and Y.-D. Yao, Surf. Sci. **507–510**, 573 (2002).
- ²⁷L. Zhang, C. Israel, A. Biswas, R. L. Greene, and A. de Lozanne, Science **298**, 805 (2002).
- ²⁸F. J. Giessibl, Science **267**, 68 (1995).
- ²⁹Y. Sugawara, M. Ohta, H. Ueyama, and S. Morita, Science **270**, 1646 (1995).
- ³⁰K. Fukui, H. Onishi, and Y. Iwasawa, Phys. Rev. Lett. **79**, 4202 (1997).
- ³¹M. Uehara, S. Mori, C. H. Chen, and S.-W. Cheong, Nature (London) **399**, 560 (1999).
- ³²M. Fäth, S. Freisem, A. A. Menovsky, Y. Tomioka, J. Aarts, and J. A. Mydosh, Science **285**, 1540 (1999).
- ³³H. Huhtinen, R. Laiho, K. G. Lisunov, V. N. Stamov, and V. S. Zakhvalinskii, J. Magn. Magn. Mater. **238**, 160 (2002).